Biosensors and Bioelectronics 24 (2008) 442–447

Contents lists available at ScienceDirect

Biosensors and Bioelectronics

journal homepage: www.elsevier.com/locate/bios

Highly ordered mesoporous carbons as electrode material for the construction of electrochemical dehydrogenase- and oxidase-based biosensors

Ming Zhou, Li Shang, Bingling Li, Lijian Huang, Shaojun Dong*

State Key Laboratory of Electroanalytical Chemistry, Changchun Institute of Applied Chemistry, Chinese Academy of Sciences, Changchun 130022, People's Republic of China

ARTICLE INFO

Article history:
Received 2 February 2008
Received in revised form 10 April 2008
Accepted 29 April 2008
Available online 4 May 2008

Keywords:
Ordered mesoporous carbons
Carbon nanotubes
Electrochemical biosensors

ABSTRACT

In this work, the excellent catalytic activity of highly ordered mesoporous carbons (OMCs) to the electrooxidation of nicotinamide adenine dinucleotide (NADH) and hydrogen peroxide (H_2O_2) was described for the construction of electrochemical alcohol dehydrogenase (ADH) and glucose oxidase (GOD)-based biosensors. The high density of edge-plane-like defective sites and high specific surface area of OMCs could be responsible for the electrocatalytic behavior at OMCs modified glassy carbon electrode (OMCs/GE), which induced a substantial decrease in the overpotential of NADH and H_2O_2 oxidation reaction compared to carbon nanotubes modified glassy carbon electrode (CNTs/GE). Such ability of OMCs permits effective low-potential amperometric biosensing of ethanol and glucose, respectively, at Nafion/ADH–OMCs/GE and Nafion/GOD–OMCs/GE. Especially, as an amperometric glucose biosensor, Nafion/GOD–OMCs/GE showed large determination range (500–15,000 $\mu mol\,l^{-1}$), high sensitivity (0.053 nA μmol^{-1}), fast (9 ± 1 s) and stable response (amperometric response retained 90% of the initial activity after 10 h stirring of 2 $mmol\,l^{-1}$ glucose solution) to glucose as well as the effective discrimination to the possible interferences, which may make it to readily satisfy the need for the routine clinical diagnosis of diabetes. By comparing the electrochemical performance of OMCs with that of CNTs as electrode material for the construction of ADH- and GOD-biosensors in this work, we reveal that OMCs could be a favorable and promising carbon electrode material for constructing other electrochemical dehydrogenase- and oxidase-based biosensors, which may have wide potential applications in biocatalysis, bioelectronics and biofuel cells.

© 2008 Elsevier B.V. All rights reserved.

1. Introduction

Recently, nanostructured electrode materials have attracted great interest, as they show better electrochemical performance than traditional materials (Wang, 2005). By combining the advantages of nanomaterials with those of carbon materials, the unique physicochemical properties of carbon nanotubes (CNTs) have paved the way to new and improved sensing devices, in general, and electrochemical biosensors, in particular (Wang, 2005). Many studies demonstrated after purification or end-opening processing, CNTs as electrode material was used to enhance the electrochemical reactivity of important biological molecules, including nicotinamide adenine dinucleotide (NADH), hydrogen peroxide (H_2O_2), ascorbic acid and etc. (Wang, 2005; Wang and Musameh, 2003). Especially, the greatly enhanced electrochemical reactivity of NADH and H_2O_2 at CNTs modified electrodes makes CNTs extremely attractive for numerous dehydrogenase- and oxidase-based biosensors (Wang, 2005). Compton and co-workers explained the observed improvement in electrochemistry at CNTs modified electrode to be the result of the presence of high edge plane density on CNTs (Banks and Compton, 2005; Banks et al., 2004,2005).

Besides the carbon materials mentioned above, highly ordered mesoporous carbons (OMCs) (Ryoo et al., 2001) have been receiving much attention owing to the extremely well-ordered pore structure, high specific pore volume and high specific surface area, which make them suitable for applications in catalysis (Joo et al., 2001), energy storage (Lee et al., 2006), and sensing etc. (Zhou et al., 2007a). Contrary to most porous silica-based materials (for example, SBA-15) that are electronic semiconductors, OMCs are intrinsic conductors. Hence, OMCs may have more interests and potential advantages for many advanced applications than other porous materials (Walcarius, 2005). Despite such potential capability of OMCs, there have been only a few studies on the electroanalytical applications (Feng et al., 2007; Jia et al., 2007; Yu et al., 2008; Zhou et al., 2007a, b,2008).

In this work, we present an advanced electrochemical biosensing platform for the detection of ethanol and glucose based on OMCs with two-dimensional (2D) hexagonal *p6mm* symmetry of the ordered pore system. The electrochemical responses of NADH and H_2O_2 were firstly studied at OMCs/GE, which exhibits more

* Corresponding author. Tel.: +86 431 85262101; fax: +86 431 85689711.
E-mail address: dongsj@ciac.jl.cn (S. Dong).

0956-5663/$ – see front matter © 2008 Elsevier B.V. All rights reserved.
doi:10.1016/j.bios.2008.04.025

favorable electron-transfer kinetics compared with CNTs/GE. Based on the greatly enhanced electrochemical reactivity of NADH and H_2O_2, Nafion/ADH–OMCs/GE and Nafion/GOD–OMCs/GE showed better electroanalytical performance to detect ethanol and glucose, respectively, compared with CNTs-based enzyme electrodes. By comparing the electrochemical performance of OMCs with that of CNTs as electrode material in this work, we reveal that OMCs showing favorable electrochemical activity could be another kind of robust and advanced carbon electrode material besides CNTs for the biosensing applications.

2. Experimental

2.1. Reagents

The OMCs were synthesized following a published procedure (Jun et al., 2000). Multiwall carbon nanotubes (purity >95%, 10–30 nm diameter) purchased from Shenzhen Nanotech. Port Co. Ltd. (China) were purified further prior to use in concentrated 1 mol l^{-1} nitric acid for 18 h by magnetic stirring. *N*, *N*′-dimethylformamide (DMF) (HPLC grade, Beijing Chemical Factory, China) were used as purchased. Glucose oxidase (GOD), alcohol dehydrogenase (ADH), bovine serum albumin (BSA) and Nafion solution (5 wt.% in 15–20% water/lower aliphatic alcohols) were purchased from Aldrich. All other chemicals were of analytical reagent grade and used as received. A 0.1 mol l^{-1} pH 7.0 phosphate buffer solution (PBS) was used in all electrochemical studies unless otherwise stated.

2.2. Apparatus

Electrochemical experiments were conducted with CHI832B electrochemical workstation. Glassy carbon electrode (GE) was used as working electrode. An Ag/AgCl electrode (saturated KCl) and a Pt wire were used as reference and counter electrode, respectively. SEM images were determined with a XL-30 ESEM. Raman spectra were recorded at ambient temperature on a Renishaw Raman system model 1000 spectrometer with at an excitation wavelength of 514.5 nm. XPS was performed on ECSALB 250. XRD patterns, nitrogen adsorption–desorption isotherms, TEM images and infrared spectrum were obtained by the instruments as reported before (Zhou et al., 2007a).

2.3. Electrode preparation and modification

Glassy carbon electrodes (3 mm diameter) were polished before each experiment with 1, 0.3 and 0.05 μm alumina powder, respectively, rinsed thoroughly with doubly distilled water between each polishing step, then washed successively with 1:1 nitric acid, acetone and doubly distilled water in ultrasonic bath and dried in air. To obtain a modifier with good properties, the ratio of OMCs (or CNTs) to DMF as well as the volume of OMCs–DMF (or CNTs–DMF) casting on GE was first optimized by AC impedance experiments in 5 mmol l^{-1} $Fe(CN)_6^{3-/4-}$ containing 0.1 mol l^{-1} KCl (data not shown), which is similar with our previous method (Liu et al., 2006). According to the experimental results, OMCs/GE (or CNTs/GE) was prepared by casting 4 μl of OMCs–DMF (or CNTs–DMF) suspension (1 ml DMF and 1 mg OMCs (or CNTs)) on GE surface, and dried under an infrared lamp.

Additionally, the experimental parameters for ADH- (or GOD-) based biosensor fabrication, such as the ratio of ADH (or GOD) to BSA, the volume of ADH–BSA (or GOD–BSA) mixture casting on OMCs/GE, CNTs/GE and GE, and the volume of Nafion casting on the electrode surface were optimized (data not shown). According to the experimental results, a 1% (wt.%) aqueous solution of BSA was mixed with the aqueous solution of ADH (or GOD) (15 mg ml^{-1}) with a volume ratio of 1:2 to give a ADH–BSA (or GOD–BSA) mixture and 6 μl of the resulting mixture was coated onto OMCs/GE, CNTs/GE and GE, respectively. A 2 μl of aqueous solution of glutaraldehyde (40 mmol l^{-1}) was further coated onto the electrodes to cross-link ADH (or GOD) onto OMCs/GE, CNTs/GE and GE, respectively, and dried at 4 °C for 2 h. Then, 2 μl Nafion was cast and dried for 1 h at 4 °C. After the modification, Nafion/ADH–OMCs/GE, Nafion/ADH–CNTs/GE and Nafion/ADH/GE (or Nafion/GOD–OMCs/GE, Nafion/GOD-CNTs/GE and Nafion/GOD/GE) were transferred to 0.1 mol l^{-1} pH 7.0 PBS for 15 min before use.

3. Results and discussion

3.1. Characterization of OMCs and CNTs

The morphologies of OMCs and CNTs were first charactered by SEM and TEM. For CNTs/GE (Fig. 1A), the surface of GE was mostly covered by homogenous CNTs with diameter between 10 and 30 nm (inset of Fig. 1A). In the SEM image of OMCs (Fig. 1B), OMCs film covering GE surface was composed of flake like particles, which have a submicron-scale particle size with the length of 0.5–1.5 μm. The TEM image of OMCs (inset of Fig. 1B) shows OMCs have a delicate and ordered surface structure. The structures

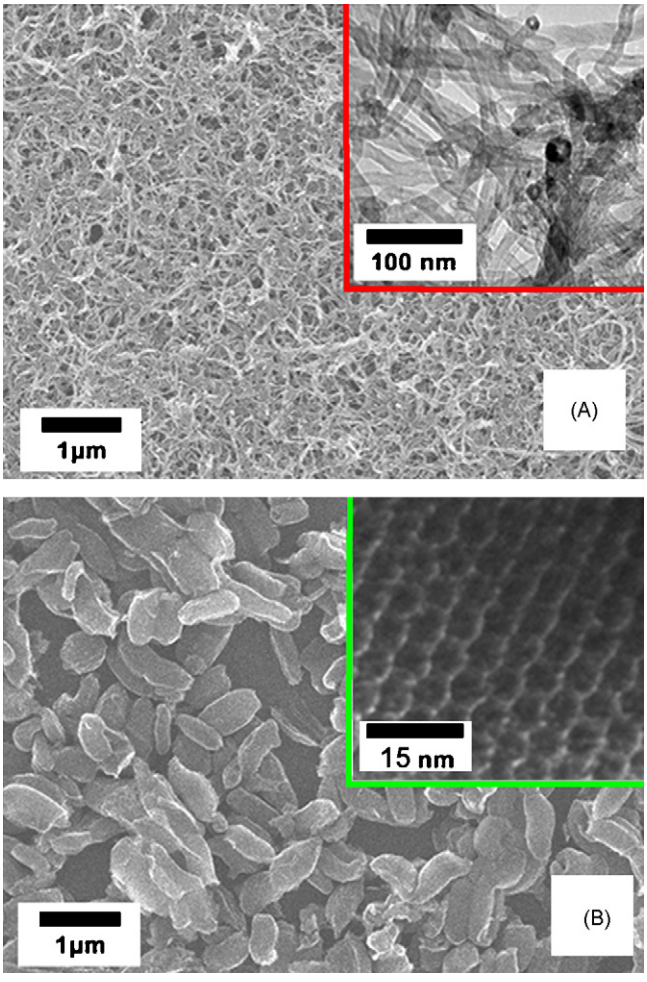

Fig. 1. (A) SEM image of CNTs/GE. Inset: TEM image of CNTs. (B) SEM image of OMCs/GE. Inset: TEM image of OMCs.

of OMCs and CNTs were further investigated by XRD and nitrogen adsorption–desorption isotherms. In Fig. S-1 (Supporting Information), the OMCs sample (a) exhibits three well-resolved peaks that can be indexed as (1 0 0), (1 1 0), and (2 0 0) reflections, which correspond to the 2D hexagonal *p6mm* symmetry of the ordered pore system. However, no obvious XRD peaks were observed for CNTs (b). The BET surface areas, total pore volumes and pore sizes of OMCs (B) are ~1038 $cm^2\ g^{-1}$, 1.66 $cm^3\ g^{-1}$ and 4.3 nm, respectively, which are much larger than those of CNTs (~203 $cm^2\ g^{-1}$, 0.43 $cm^3\ g^{-1}$ and 2.1 nm, respectively).

The oxygen-containing functional groups (OFGs) are presented both on the surfaces of OMCs and CNTs, which were confirmed by FT-IR and XPS in Fig. S-2 (Supporting Information). As shown in the FT-IR spectra (A), the band around 3435, 1688, 1550, 1515 and 1106 cm^{-1} are attributed to the OFGs on CNT and OMC. XPS spectra (B) show the O/C ratio from XPS for CNTs and OMCs is 0.098 and 0.032, respectively. This means CNTs contained more OFGs than OMCs. To obtain further information on the structure and topology of OMCs and CNTs, Raman spectroscopy was carried out. In Fig. S-2 (Supporting Information), the Raman spectrum of CNTs (e) exhibits the presence of D and G bands. The D band at 1348 cm^{-1} arises from sp^3-hybridized carbon, and the peak at 1595 cm^{-1} represents the optically allowed E_{2g} zone center mode of crystalline graphite (Ferrari and Robertson, 2000; Jia et al., 2007). This means the relative intensity ratio of the D and G lines (I_D/I_G ratio) is proportional to the number of defect sites in carbon materials (Ferrari and Robertson, 2000; Jia et al., 2007). Raman spectra show the I_D/I_G ratio of OMCs (f) and CNTs (e) is 1.82 and 0.58, respectively. This means, without purification or end-opening processing (which are usually in CNTs applications), OMCs contains more edge-plane-like defective sites (EDSs) than CNTs.

3.2. Electron-transfer kinetics at different electrodes

The capability of electron transfer on OMCs/GE, CNTs/GE and GE surface was investigated by AC impedance experiments in Fig. 2. The Randles circuit (inset of Fig. 2) is chosen to fit the obtained impedance data. The resistance to charge transfer (R_{ct}) and the diffusion impedance (W) are both in parallel to the interfacial capacitance (C_{dl}). The diameter of the semicircle corresponds to the interfacial electron-transfer resistance (R_{ct}) (Liu et al., 2006). By fitting the data, R_{ct} can be estimated to be 213.6 Ω at GE (a). While the R_{ct} decreases to 95.2 Ω arising from the accelerating of electron transfer by CNTs (b). When OMCs were modified on GE, the R_{ct} decreases to 13.2 Ω (c) revealing the much lower electron-transfer resistance on OMCs/GE compared with that on CNTs/GE. These results demonstrate that OMCs can form good electron pathway between the electrode and electrolyte and presence of OMCs made the electron transfer easier compared with that of CNTs.

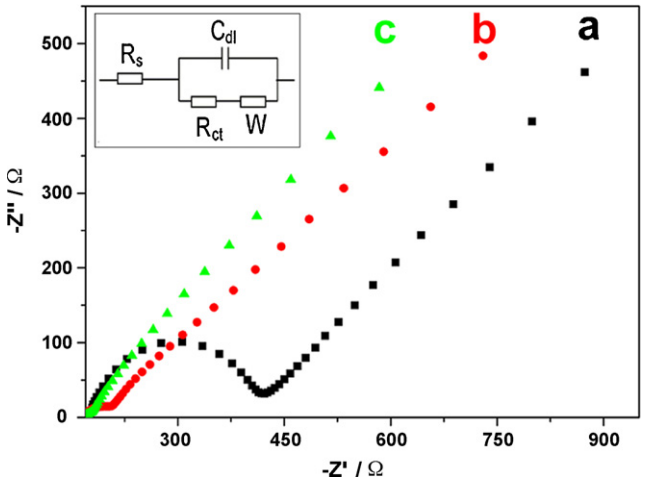

Fig. 2. Nyquist plots at GE (a), CNTs/GE (b) and OMCs/GE (c) in 5 mmol l^{-1} $Fe(CN)_6^{3-/4-}$ containing 0.1 mol l^{-1} KCl. Inset is the equivalent circuit. The frequency range is from 1 Hz to 10 kHz. Inset is the equivalent circuit.

3.3. Electrooxidation of NADH and hydrogen peroxide and their detection

In Fig. 3A–C, the cyclic voltammograms (CVs) for NADH oxidation at different electrodes were compared. With GE (Fig. 3A), the oxidation results in an anodic peak at +0.65 V. For CNTs/GE (Fig. 3B), it exhibits an obvious decrease (0.20 V) in overpotential with 2.44-fold increase in peak current for NADH oxidation compared with GE. In Fig. 3C, the catalytic activity of OMCs/GE is evident from a marked decrease (0.20 V) in overpotential as well as 2.35-fold current increase and for NADH oxidation compared to CNTs/GE. Obviously, the presence of OMCs made the electron transfer much easier compared with that of CNTs. Raman spectra (Fig. S-2C (Supporting Information)) indicate OMCs contains more EDSs than CNTs. This means the more EDSs on OMCs should be mainly responsible for the enhanced catalytic activity at OMCs/GE compared with that at CNTs/GE (Banks and Compton, 2005; Banks et al., 2004,2005). Additionally, the nanostructured channel surface of OMCs with large surface area may make an increase on the apparent electroactive surface area of OMCs/GE, which could offer a favorite microenvironment for transferring species in solution through the pores of OMCs, and also would be beneficial for accelerating electron transfer between the electrode and species in solution. Furthermore, the uniform pore size, ordered arrangement of carbon nanorods and pieces of OMCs homogeneously covered on GE (Fig. 1B) could be very attractive for various electrochemical applications, especially for the development of electrochemical sensors and biosensors.

Under the potential of NADH oxidation at each electrode, the analytical performance of OMCs/GE, CNTs/GE and GE for NADH detection in 0.1 mol l^{-1} pH 7.0 PBS was investigated. As shown in Fig. 4A and Table S-1 (Supporting Information), compared with CNTs/GE and GE, OMCs/GE exhibits faster response time, wider linear range, lower detection limit and higher sensitivity. Additionally, an extremely attractive feature of OMCs modified electrode is its highly stable amperometric NADH response (data not shown). For OMCs/GE (with the applied potential of +0.25 V), the NADH amperometric response of the initial activity remained 87% after 90 min stirring of 0.4 mmol l^{-1} NADH solution which is more stable compared to 70% at CNTs/GE (at +0.45 V) and 36% at GE (at +0.65 V), indicating the better resistance to fouling of the oxidation process at OMCs/GE. It has been reported the presence of polar OFGs should be responsible for the adsorption, fouling and deactivation at carbon-based electrodes (Rao et al., 1999). The O/C ratio of GE polished in alumina/water slurry is 0.14 (Chen and McCreery, 1996), which is more than that of OMCs (0.032) and CNTs (0.098) (Fig. S-2B (Supporting Information)). This suggests the less OFGs on OMCs compared with those on CNTs and GE could be partially responsible for the minimizing passivation effects at OMCs/GE (Rao et al., 1999). Compton and co-workers reported the high density of EDSs on the carbon materials may result in the effect of resistance to fouling at carbon-based electrodes (Banks and Compton, 2005). This means the more EDSs on OMCs compared with those on CNTs (Fig. S-2 (Supporting Information)) could play an important role in minimizing passivation effects for NADH oxidation at OMCs/GE. Additionally, another important aspect for eliminating

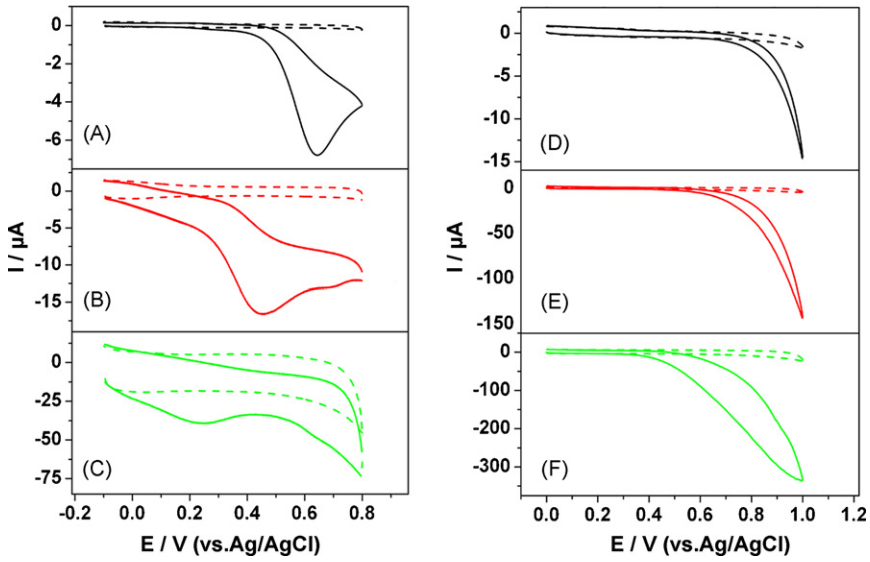

Fig. 3. CVs for 2 mmol l^{-1} NADH at GE (A), CNTs/GE (B) and OMCs/GE (C). CVs for 4.2 mmol l^{-1} H_2O_2 at GE (D), CNTs/GE (E) and OMCs/GE (F). Dotted lines represent the background response. Scan rate: 50 mV s^{-1}.

surface fouling effects is the improved electron-transfer kinetics and more negative potential applied for the electrooxidation of NADH at OMCs/GE, which can limit the amount of radical intermediates and their dimerization. Furthermore, the 2D ordered mesoporous structures of OMCs are expected to be advantageous efficient diffusion and transport of reactants and by-products in the application of electrochemical sensors (Chang et al., 2007; Zhou et al., 2008).

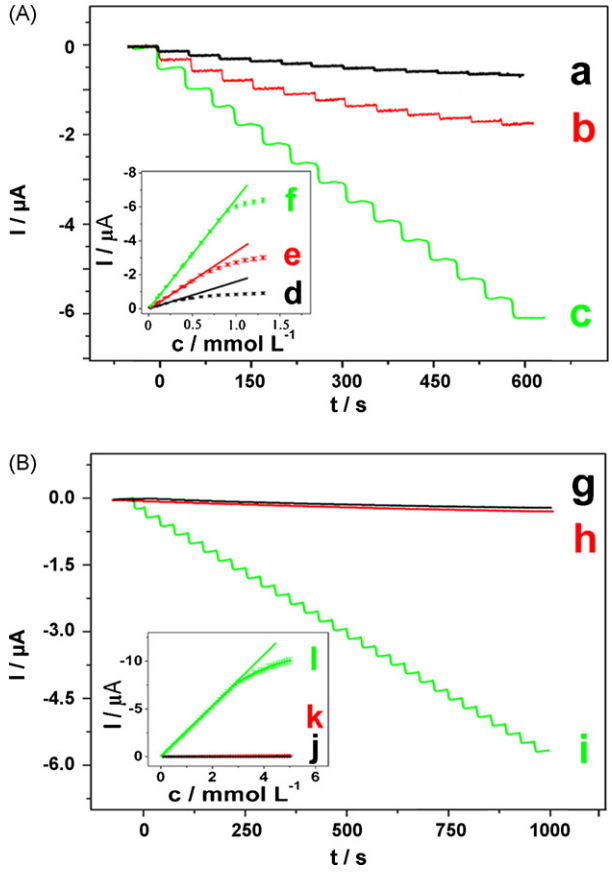

Fig. 4. (A) Current–time curves for GE (at +0.65 V, (a), CNTs/GE (at +0.45 V (b)) and OMCs/GE (at +0.25 V (c)) with successive addition of 0.1 mmol l^{-1} NADH. Inset: calibration curves for NADH at GE (d), CNTs/GE (e) and OMCs/GE (f). (B) Current–time curves for GE (g), CNTs/GE (h) and OMCs/GE (i) at +0.35 V with successive addition of 0.1 mmol l^{-1} H_2O_2. Inset: calibration curves for H_2O_2 at GE (j), CNTs/GE (k) and OMCs/GE (l).

Fig. 3D–F showed the CVs of different electrodes in the presence of H_2O_2. With the addition of H_2O_2 to the solution, the anodic current began increasing from +0.30, +0.50 and +0.70 V at OMCs/GE, CNTs/GE and GE, respectively. This suggests OMCs/GE exhibits a higher electrocatalytic activity for H_2O_2 oxidation compared with CNTs/GE and GE, which may result from the unique microstructure of OMCs with large density of EDSs and large surface area (Banks et al., 2004). Hence, the marked decrease in the overvoltage for the H_2O_2 reaction allows the convenient low-potential amperometric detection. Fig. 4B shows the amperometric responses of OMCs/GE, CNTs/GE and GE to successive additions of H_2O_2 at +0.35 V, and Table S-1 (Supporting Information) summarizes the analytical parameters for H_2O_2 detection on the corresponding electrodes. As shown, OMCs/GE responds very rapidly (5 ± 1 s) and favorably to these changes in the peroxide concentration, however, no obvious response is observed in analogous measurements at CNTs/GE and GE. Obviously, as a low-potential amperometric sensor for H_2O_2 detection, OMCs/GE exhibits faster response time and higher sensitivity compared with CNTs/GE and GE.

The possible interferences of 0.2 mmol l^{-1} AA, GSH, DA, UA or EP show significantly interferences to 2 mmol l^{-1} NADH (or H_2O_2) detection on OMCs/GE, CNTs/GE and GE. Coating a thin film of Nafion polymer as an effectively perselective barrier on OMCs/GE may eliminate the interferences (Wang et al., 2003). After being stored at 4 °C for 1 month, current losses 7.0% (or 8.0%) at OMCs/GE and 20% (or 30%) at GE for the amperometric response of 0.1 mmol l^{-1} NADH (or H_2O_2). This indicates OMCs/GE could be used as a stable sensor for NADH (or H_2O_2) detection.

3.4. Toward biosensing applications based on the electrooxidation of NADH and hydrogen peroxide

The greatly enhanced electrochemical reactivity of NADH and H_2O_2 at OMCs/GE compared with CNTs/GE makes OMCs extremely attractive for dehydrogenase- and oxidase-based amperometric

biosensors, which has been illustrated in connection to amperometric measurements of ethanol and glucose in this work.

In order to obtain the best amperometric ethanol responses, the applied potentials at ADH-based electrodes for ethanol detection were first optimized (data now shown). The amperometric response for ethanol at Nafion/ADH/GE, Nafion/ADH–CNTs/GE and Nafion/ADH–OMCs/GE reached a maximum value at +0.80, +0.60 and +0.40 V, respectively. So we choose +0.80, +0.60 and +0.40 V as the applied potential for Nafion/ADH/GE, Nafion/ADH–CNTs/GE and Nafion/ADH–OMCs/GE, respectively. As shown in Fig. 5A and Table S-1 (Supporting Information), Nafion/ADH–OMCs/GE exhibits faster response time, wider linear range and lower detection limit for ethanol detection compared with Nafion/ADH–CNTs/GE and Nafion/ADH/GE. The relevant physiological levels of 0.2 mmol l^{-1} AA, EP or UA did not show interferences to ethanol detection (2 mmol l^{-1}) at pH 7.0 on Nafion/ADH–OMCs/GE, Nafion/ADH–CNTs/GE and Nafion/ADH/GE (data not shown), where Nafion acted as effectively perselective barriers (Wang et al., 2003). The reproducibility of Nafion/ADH–OMCs/GE was also tested. The experiments were run at six Nafion/ADH–OMCs/GE, and the results demonstrated Nafion/ADH–OMCs/GE possesses a good reproducibility with a relative standard deviation of 4.3% for 1 mmol l^{-1} ethanol.

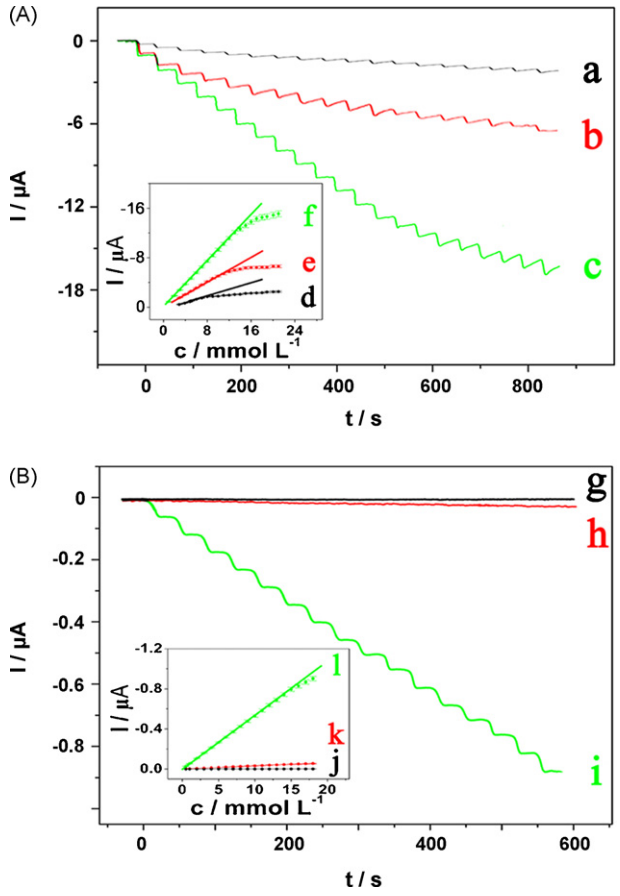

Fig. 5. (A) Current–time curves for Nafion/ADH/GE (at +0.80 V (a)), Nafion/ADH–CNTs/GE (at +0.60 V (b)) and Nafion/ADH–OMCs/GE (at +0.40 V (c)) with successive addition of 1 mmol l^{-1} ethanol. Inset: calibration curves for ethanol at Nafion/ADH/GE (d), Nafion/ADH–CNTs/GE (e) and Nafion/ADH–OMCs/GE (f). Electrolyte: air-saturated 0.1 mol l^{-1} pH 7.0 PBS without being purged by nitrogen. (B) Current–time curves for Nafion/GOD/GE (g), Nafion/GOD-CNTs/GE (h) and Nafion/GOD–OMCs/GE (i) at +0.35 V with successive addition of 1 mmol l^{-1} glucose. Inset: calibration curves for glucose at Nafion/ADH/GE (j), Nafion/ADH–CNTs/GE (k) and Nafion/ADH–OMCs/GE (l). Electrolyte: 0.1 mol l^{-1} pH 7.0 PBS containing 10 mmol l^{-1} NAD^+.

Another extremely attractive feature of OMCs is that it could be used as a kind of advanced matrix, which makes Nafion/GOD–OMCs/GE as a promising candidate of the efficient biosensors for fast, stably and continuously measure plasma glucose level for the clinical diagnosis of diabetes. Fig. 5B displays the current–time responses of Nafion/GOD–OMCs/GE, Nafion/GOD-CNTs/GE and Nafion/GOD/GE for glucose detection at pH 7.0 with the applied potential of +0.35 V, and Table S-1 (Supporting Information) summarizes the analytical parameters at different electrodes. As shown, both of Nafion/GOD/GE (g) and Nafion/GOD-CNTs/GE (h) do not respond obviously to the glucose additions. Yet, the OMCs-based GOD-biosensor offers substantially larger signals reflecting the better electrocatalytic activity of Nafion/GOD–OMCs/GE (i). For Nafion/GOD–OMCs/GE, the good linear ranges are from 0.5 to 15 mmol l^{-1} (correlation coefficient of 0.995) for glucose detection with a sensitivity of 0.053 μA mmol l^{-1} and a detection limit of 156.52 μmol l^{-1} (S/N = 3). This suggests Nafion/GOD–OMCs/GE constructed in this work may readily satisfy the need for the routine clinical diagnosis of diabetes by the fasting plasma glucose or the oral glucose tolerance test suggested by the American Diabetes Association (Davidson, 2001). The current response of Nafion/GOD–OMCs/GE generally reached a steady-state level with 9 ± 1 s after the glucose addition, and the amperometric response retained 90% of the initial activity after 10 h stirring of 2 mmol l^{-1} glucose solution (data not shown). This indicates the response to glucose at Nafion/GOD–OMCs/GE was fast and highly stable, which may make Nafion/GOD–OMCs/GE as a fast and highly stable biosensor to continuously measure the plasma glucose level for the diagnosis of diabetes. While a well-defined glucose (10 mmol l^{-1}) response is observed at Nafion/GOD–OMCs/GE using a potential of +0.35 V, relevant physiological levels of AA (0.2 mmol l^{-1}), EP (0.2 mmol l^{-1}) and UA (0.2 mmol l^{-1}) result in negligible signals (data not shown) due to the Nafion polymer as an effectively perselective barrier (Wang et al., 2003), which means Nafion/GOD–OMCs/GE could be applied in the clinical diagnosis of diabetes. The reproducibility of Nafion/GOD–OMCs/GE was also tested. The experiments were run at six Nafion/GOD–OMCs/GE, and the result demonstrates Nafion/GOD–OMCs/GE has a good reproducibility with a relative standard deviation of 2.18% for 1 mmol l^{-1} glucose. The large determination range, high sensitivity, fast and stable response to glucose as well as the effective discrimination of Nafion/GOD–OMCs/GE to the possible interferences may make Nafion/GOD–OMCs/GE as a promising candidate of the efficient biosensors for fast, stably and consecutively monitoring plasma glucose level for the clinical diagnosis of diabetes.

After being stored at 4 °C for 1 month, 9.3% current loss at Nafion/ADH–OMCs/GE (or 7.0% at Nafion/GOD–OMCs/GE) was observed by the amperometric response of 1 mmol l^{-1} ethanol (or glucose). This means OMCs-based ADH (or GOD) biosensors could be used as stable sensor for ethanol (or glucose) detection, which could be attributed to the interaction between OMCs and enzymes. The hydrophobic interactions between carbon-based materials and enzymes are widely accepted (Shim et al., 2002; Wen et al., 2007). OMCs material is a kind of carbon-based materials, so the enzyme (ADH or GOD) may also be immobilized on OMCs via the hydrophobic interactions. In the mean time, physical adsorption of ADH (or GOD) onto OMCs should not be ignored. As a comparison, we studied the adsorption of ADH (or GOD) on OMCs/GE. The results display that the adsorption amount continuously increases with the immersing time and does not reach saturation even after 24 h (data not shown). However, the ADH/OMCs (or GOD/OMCs) films are not stable, and they can easily shed from the electrode. These results suggest ADH (or GOD) may also interact with OMCs by the physical adsorption, and it is necessary to use Nafion as a binder to

hold the ADH (or GOD) stably kept on the electrode surface in this work.

From the demonstration above we may conclude that OMCs-based enzyme (ADH and GOD) biosensors constructed in work shows better analytical performance for ethanol and glucose detection compared with CNTs-based enzyme biosensors, and these advantages of OMCs-based enzyme biosensors can be explained by the effective transfer of substrate and products through OMCs matrixes containing enzymes, resulting from the unique physicochemical properties of OMCs. Thus, as a kind of more advanced amperometric transducer compared with CNTs, OMCs could be a better choice for electrochemical biosensors for substrates of other dehydrogenase and oxidase enzymes and other practical applications.

4. Conclusions

In this work, the characterization and application of OMCs/GE for the preparation of electrochemical dehydrogenase- and oxidase-based biosensors are proposed. The comparison of the response at OMCs/GE, CNTs/GE and GE for the electrocatalysis of NADH and H_2O_2 suggests that OMCs/GE has more favorable electron-transfer kinetics than CNTs/GE and GE. Based on the greatly enhanced electrochemical reactivity of NADH and H_2O_2 at OMCs/GE, Nafion/ADH–OMCs/GE and Nafion/GOD–OMCs/GE showed better analytical performance for biosensing ethanol and glucose, respectively, compared with CNTs-based dehydrogenase- and oxidase-biosensors. These may make OMCs to be another "popular" carbon electrode material for constructing electrochemical biosensing platform based on dehydrogenase- and oxidase enzymes besides CNTs.

Acknowledgement

This research was supported by the National Natural Science Foundation of China (nos. 20575064 and 20675076).

Appendix A. Supplementary data

Supplementary data associated with this article can be found, in the online version, at doi:10.1016/j.bios.2008.04.025.

References

Banks, C.E., Compton, R.G., 2005. Analyst 130 (9), 1232–1239.
Banks, C.E., Moore, R.R., Davies, T.J., Compton, R.G., 2004. Chemical Communications 16, 1804–1805.
Banks, C.E., Davies, T.J., Wildgoose, G.G., Compton, R.G., 2005. Chemical Communications 7, 829–841.
Chang, H., Joo, S.H., Pak, C., 2007. Journal of Materials Chemistry 17, 3078–3088.
Chen, P., McCreery, R.L., 1996. Analytical Chemistry 68 (22), 3958–3965.
Davidson, M.B., 2001. Diabetes Spectrum 14 (2), 67–71.
Feng, J.-J., Xu, J.-J., Chen, H.-Y., 2007. Biosensors and Bioelectronics 22 (8), 1618–1624.
Ferrari, A.C., Robertson, J., 2000. Physical Review B – Condensed Matter and Materials Physics 61 (20), 14095.
Jia, N., Wang, Z., Yang, G., Shen, H., Zhu, L., 2007. Electrochemistry Communications 9 (2), 233–238.
Joo, S.H., Choi, S.J., Oh, I., Kwak, J., Liu, Z., Terasaki, O., Ryoo, R., 2001. Nature 412 (6843), 169–172.
Jun, S., Joo, S.H., Ryoo, R., Kruk, M., Jaroniec, M., Liu, Z., Ohsuna, T., Terasaki, O., 2000. Journal of the American Chemical Society 122 (43), 10712–10713.
Lee, J., Kim, J., Hyeon, T., 2006. Advanced Functional Materials 18 (16), 2073–2094.
Liu, Y., Qu, X., Guo, H., Chen, H., Liu, B., Dong, S., 2006. Biosensors and Bioelectronics 21 (12), 2195–2201.
Rao, T.N., Yagi, I., Miwa, T., Tryk, D.A., Fujishima, A., 1999. Analytical Chemistry 71 (13), 2506–2511.
Ryoo, R., Joo, S.H., Kruk, M., Jaroniec, M., 2001. Advanced Functional Materials 13 (9), 677–681.
Shim, M., Shi Kam, N.W., Chen, R.J., Li, Y., Dai, H., 2002. Nano Letter 2 (4), 285–288.
Walcarius, A., 2005. Comptes Rendus Chimie 8 (3–4), 693–712.
Wang, J., 2005. Electroanalysis 17 (1), 7–14.
Wang, J., Musameh, M., 2003. Analytical Chemistry 75 (9), 2075–2079.
Wang, J., Musameh, M., Lin, Y., 2003. Journal of the American Chemical Society 125 (9), 2408–2409.
Wen, D., Liu, Y., Yang, G., Dong, S., 2007. Electrochimica Acta 52 (16), 5312–5317.
Yu, J., Yu, D., Zhao, T., Zeng, B., 2008. Talanta 74 (5), 1586–1591.
Zhou, M., Ding, J., Guo, L.P., Shang, Q.K., 2007a. Analytical Chemistry 79 (14), 5328–5335.
Zhou, M., Guo, L.-P., Lin, F.-Y., Liu, H.-X., 2007b. Analytica Chimica Acta 587 (1), 124–131.
Zhou, M., Guo, L.-P., Hou, Y., Peng, X.-J., 2008. Electrochimica Acta 53 (12), 4176–4184.